

Ecological Stability Emerges at the Level of Strains in the Human Gut Microbiome

Richard Wolff¹, William Shoemaker¹, Nandita Garud^{1,2,*},

1 Department of Ecology and Evolutionary, UCLA

2 Department of Human Genetics, UCLA

* ngarud@g.ucla.edu

Abstract

The human gut microbiome is a complex community that harbors substantial ecological diversity at the species level, as well as at the strain level within species. In healthy hosts, species abundance fluctuations in the microbiome community are thought to be stable, and these fluctuations can be described by macroecological laws. However, it is less clear how strain abundances change over time. An open question is whether individual strains behave like species themselves, exhibiting stability and following the macroecological relationships known to hold at the species level, or whether strains have different dynamics, perhaps due to the relatively close phylogenetic relatedness of co-colonizing lineages. In this study, we sought to characterize the typical strain-level dynamics of the healthy human gut microbiome on timescales ranging from days to years. We show that genetic diversity within almost all species is stationary, tending towards a long-term typical value within hosts over time scales of several years, despite fluctuations on shorter timescales. Moreover, the abundance fluctuations of strains can be sufficiently described by a stochastic logistic model (SLM) – a model previously used to describe abundance fluctuations among species around a fixed carrying capacity – in the vast majority of cases, suggesting that strains are dynamically stable. Lastly, we find that strain abundances follow the same macroecological laws known to hold at the species level. Together, our results suggest that macroecological properties of the human gut microbiome, including its stability, emerge at the level of strains.

Introduction

The human gut microbiome is composed of a diverse array of microbial species. While a typical gut microbial species harbors considerable genetic variation both within and across hosts, the ecological and functional consequences of this diversity remain largely unknown. Although recent efforts have begun to characterize how genotypic diversity changes within healthy hosts over months to years, these trends are not, at present, quantified on the short time frames most relevant for microbial ecology – that is, over periods of days [5, 10, 15, 24, 25, 28, 30]. Understanding the typical scale of daily fluctuations in genetic variation is critical to assessing both the long-term stability of the genetic composition of the gut

microbiome, as well the effects of occasional large perturbations resulting from changes in host diet, 26
medication, travel, illness, and other factors. 27

Two kinds of processes drive within-host changes in genetic variation in the human gut. First, there 28
is the evolutionary modification of resident lineages, which can result in small numbers ($O(1) - O(10)$) of 29
single nucleotide variants (SNVs) sweeping from low to high frequency on timescales of weeks to months. 30
Second, fluctuations in the abundance of strains, which have a typical nucleotide divergence of 1%, can 31
result in large numbers ($\sim O(10^4)$) of SNV frequency changes over time [10].. The most dramatic 32
manifestation of this second process is strain replacement, when one strain of a species invades and drives 33
the resident to extinction, though such events are infrequent over ~ 1 year timescales [24, 25]. Thus, strain 34
abundance fluctuations have several orders of magnitude greater impact on intraspecies genetic variation 35
over time than evolutionary changes. 36

Prior analyses have demonstrated that the majority of strains persist within hosts over a period of at 37
least several years [5, 15, 24, 25]. Moreover, strains can be resilient to even large perturbations of the gut 38
community, such as antibiotics [23] and fecal microbiome transplants (FMT) [11]. Interestingly, strains in 39
the gut microbiome frequently co-exist with a handful of other strains belonging to the same species. This 40
“oligo-colonization” model – in which a species is made up of $\sim 1 - 4$ strains [10, 54] – has been observed in 41
a number of other host-associated microbiota, both at different human body sites [42] as well as in other 42
organisms [8, 16]. 43

The coexistence of multiple strains within an individual gut for periods of years contrasts starkly 44
with the rapid evolution known to occur regularly at individual SNVs. This suggests that while 45
competitive exclusion and directional selection may frequently prevail among closely related lineages, 46
highly diverged lineages are generally subject to different eco-evolutionary forces. That is, while SNVs are 47
known to frequently arise and fix within populations, strains, which are far more genetically diverged, seem 48
much less likely to drive other strains extinct. 49

To understand the typical abundance fluctuations of strains in the microbiome, we leverage concepts 50
from macroecology. Macroecology focuses on elucidating the statistical and ecological properties of 51
communities. There is an increasing body of work which demonstrates that patterns of microbial species 52
abundance and diversity follow macroecological laws across disparate environments, including the human 53
gut [1, 6, 14, 45]. Surprisingly, many of these macroecological laws can be recapitulated through intuitive 54
ecological models containing few if any free parameters [1, 6, 44]. Among these successful models is the 55
Stochastic Logistic Model (SLM), which describes the dynamics of a population experiencing rapid 56
environmental fluctuations around a fixed carrying capacity. Whether the strains making up a community 57
exhibit regular, statistically quantifiable dynamics, and if so, whether these dynamics can be explained 58
using simple models, are fundamentally macroecological questions. 59

In this study, we examine whether the macroecological dynamics observed at the species level hold at 60
the strain level. We investigate the temporal dynamics and macroecology of strains in a densely sampled 61
cohort of four healthy, adult hosts (*am*, *an*, *ao*, and *ae*) from a previously published data set [21]. We find 62
that the vast majority of strains in the human gut are stable in these healthy hosts on ~ 1 year time scales, 63
and that they exhibit some of the same macroecological patterns as species. We approached the problem of 64
intraspecies stability first by quantifying the change in genetic polymorphism through time, and showed 65
that levels of intra-species genetic variation (as measured by the nucleotide diversity π) fluctuate around 66
long-term steady state values. Next, we connected the lack of directionality exhibited by genetic diversity 67
through time with an underlying model of stable population dynamics among—the SLM, first applied 68

by [1, 6] to characterize microbial diversity at the species level. We find that this model provides a sufficient description of strain dynamics in almost all cases, and that it fails in the only case of a clear strain “replacement” in our cohort. Lastly, we demonstrated that several macroecological laws initially shown to hold at the species level also hold among strains. Together, this work indicates that the stability of the gut microbiome emerges at the level of individual strains.

Results

Stability of intraspecies diversity

Fluctuations in intraspecies genetic diversity reflect both the population genetic forces affecting lineages within a population and the ecological forces affecting the relative abundances of different strains. To investigate these forces, we first analyzed the nucleotide diversity of species in our cohort.

An illustrative example of these temporal dynamics is provided by *Bacteroides vulgatus*, the most abundant species in host *am*. In **Figure 1A**, nucleotide diversity π for this population is plotted over the two-year sampling period. While π undergoes relatively large fluctuations (varying by more than a factor of two), there is no apparent trend for diversity to systematically either increase or decrease. Rather, π seems to fluctuate around a characteristic value of about 1.5×10^{-3} , with periods of elevated or decreased diversity followed by a return to the “steady” state. Across all species examined, nucleotide diversity typically ranged from approximately $10^{-4} - 10^{-2}$ per basepair.

We implemented a permutation test to determine quantitatively if levels of diversity were indeed constant through time for species in our data (Methods). Applying this test, we found that 55 of the 64 species for which SNPs could reliably be inferred (including *B. vulgatus* in *am*) showed no trend in π throughout the sampling period at a 5% significance level, confirming our initial qualitative assessment of the overall stationarity of genetic diversity (Supplementary Figure 1).

Levels of nucleotide diversity in many species in our data are inconsistent with the presence of a single strain, or of a group of lineages which diversified since entering the host. Using conservatively high estimates for per-site mutation rates, generation times, and time since colonization, the authors of [?] estimated that genetic polymorphism could reach values of at most about 10^{-3} per basepair if lineages diverged within a host. If however, a species is made up of multiple strains that accumulated mutations for many generations before colonizing the same gut community, nucleotide diversity can easily surpass this value.

The nucleotide diversity of *B. vulgatus* hovers just above this upper threshold, indicating that the species may be made up of multiple diverged strains. To assess this, we inferred the underlying strain structure *B. vulgatus* (**Figure 1B**). While accurate strain inference is inherently limited in cases where read depth is low, distinct strains can be confidently inferred when SNV data is available at many timepoints. Using a previously published algorithm which leverages the correlations in allele frequency trajectories between linked variants to detect strains in dense longitudinal data, we were able to separate out two distinct clusters of allele frequency trajectories, strongly indicating that *B. vulgatus* is oligo-colonized by a mixture of three strains (Supplementary Figure 2). As with π , the relative abundances of the strains seem centered around a fixed steady state, to which the strains return following transient increases or decreases in abundance. Indeed, variations in the relative abundances of the strains away from their steady state (e.g. around timepoint 100, when one strain rises markedly in abundance) correspond

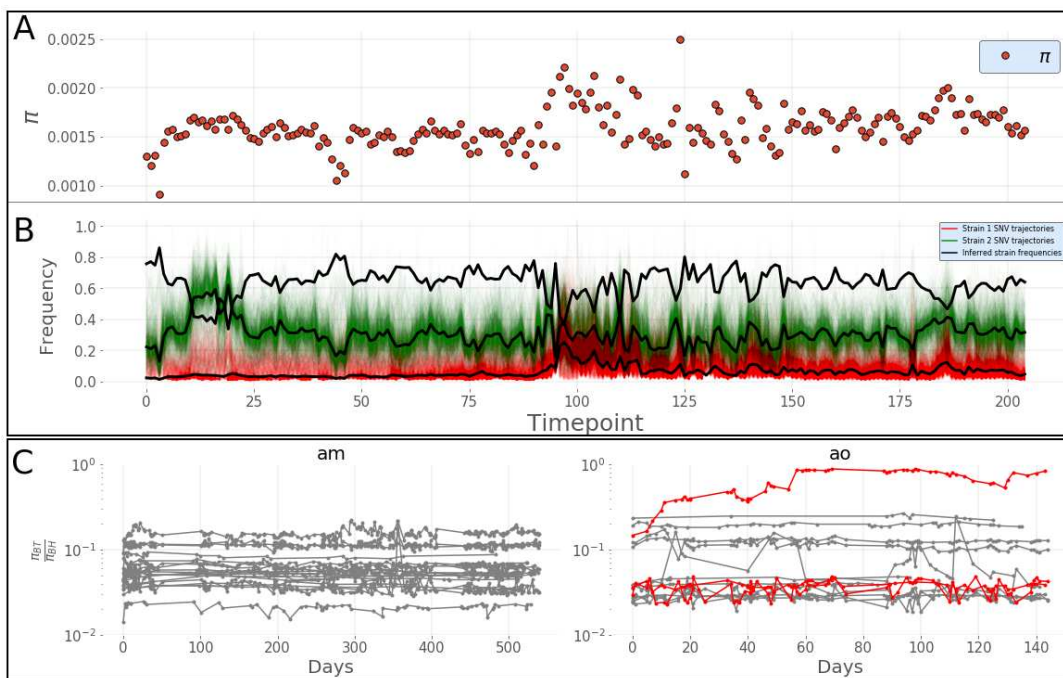


Figure 1. **A)** Nucleotide diversity π of *Bacteroides vulgatus* in host *am*. Short term fluctuations in diversity tend ultimately to revert to a long term average value. **B)** Results of strain inference for *B. vulgatus*. Each colored line represents the trajectory of a single phased allele, while the color itself denotes the strain cluster the allele was identified as belonging to (the unphased allelic trajectories can be seen in Supplementary Figure 2.) Black lines are centroids of the allele trajectory clusters, and are an estimator for the true relative abundance of the strain. Fluctuations in strain frequency are mirrored by fluctuations in genetic diversity. Note the x-axis shows the ordinal timepoint number, not number of days. **C)** Trajectories of the ratio of π_{BT} to π_{BH} for each species in hosts *am* and *ao*. The bulk of trajectories are grey, indicating no significant trend across the sampling period; red trajectories are those which show a significant positive trend. π_{BT} approaches π_{BH} for *F. prausnitzii* in host *ao*, indicating a possible partial displacement.

exactly to perturbations in π . It is clear in this case that the changes in strain abundance are in fact the leading contribution to fluctuations in intraspecies genetic diversity.

Nucleotide diversity π can, in theory, remain relatively constant even when there are dramatic changes in the strain-level composition of a species—this might happen if, for instance, a species colonized by a single strain was replaced by another single strain from a different host. However, such changes would manifest in the genetic composition of the species changing dramatically, with the level of diversity between timepoints approaching or exceeding that between hosts, as unrelated hosts typically contain distinct, highly diverged sets of strains [24]. To understand how the genetic composition of species changes in time, we computed the nucleotide diversity between timepoints π_{BT} , normalizing this quantity by the average genetic diversity between hosts π_{BH} (Methods). We again conducted a permutation test on π_{BT} time series, and found significant temporal trends in diversity change in just four species. Intriguingly, three of these four species were found in a single host (*ao*). Among all species in all hosts, the ratio $\frac{\pi_{BT}}{\pi_{BH}}$ approached one only for *Faecalibacterium prausnitzii* in host *ao* (Figure 1C, right, in red).

Stochastic logistic model

Next, we sought to determine if the temporal dynamics of strains could be captured using a naive model. Recent work in microbial ecology has repeatedly demonstrated the power of such models to reproduce qualitative and quantitative features of natural microbial community dynamics [1, 6, 43, 44]. We show that the stochastic logistic model (SLM), a minimal model itself requiring the fit of no free parameters, is a good fit for nearly all the strain time series in our cohort.

We first obtained time series of strain abundances. To do so, we determined the relative frequencies of strains using the technique described above, and then multiplied these by the frequencies of the species to which they belong, excluding species and samples with low abundance (Methods).

If x_i is the abundance of strain i which follows an SLM, then:

$$\frac{dx_i}{dt} = \frac{x_i}{\tau_i} \left(1 - \frac{x_i}{K_i}\right) + \sqrt{\frac{\sigma_i}{\tau_i}} x_i \eta(t)$$

here τ_i is the intrinsic growth rate of the strain and $\eta(t)$ is a Brownian noise term. Under the assumptions of the model, each population has a long-term carrying capacity K_i , and temporal fluctuations in abundance around this value are driven entirely by environmental noise with amplitude determined by σ_i . Populations may experience large fluctuations in abundance over short timescales, and may even be temporarily found far from their long-term average value, but these fluctuations will be transient. Over long timescales, the stationary distribution in abundances predicted by the SLM is the following Gamma distribution [1]:

$$\rho(x_i) = \frac{1}{\Gamma(2\sigma_i^{-1} - 1)} \left(\frac{2}{K_i \sigma_i}\right)^{2\sigma_i^{-1} - 1} x^{2\sigma_i^{-1} - 2} \exp\left(-\frac{2}{K_i \sigma_i} x\right) \quad (2)$$

In Figure 2A, simulations from the SLM are compared with the actual time series of two strains. The qualitative agreement between data and model is evident, and is further reflected in the close match of the empirical distributions of abundances over the whole sampling period with the predicted stationary Gamma distribution.

To assess quantitatively whether the time series of populations in our cohort could be adequately described by an SLM, we developed and implemented a goodness-of-fit test (Methods). The test determines whether the transitions between subsequent timepoints are consistent with an SLM.

The SLM fit the data in the overwhelming majority of cases: 94% across all hosts combined (Figure 2B), with similar percentages of strains fitting the model in each host. We emphasize that this test did not require the fit of any free parameters, as the parameters of the SLM associated with each population were estimated only from the mean and variance in its abundance (Methods). The agreement of data and model is thus unlikely to be an artifact of model over-specification.

The SLM was rejected in some instances. Notably, the model was rejected for one of the two strains of *F. prausnitzii* in *ao*, the same species which was shown above to have experienced a large, directional change in its genetic diversity and composition. This strain experienced a rapid decrease in abundance midway through the sampling period, and thereafter never fully recovered to its previous state (Supplemental Figure 3). The other strain fit the SLM. We conclude that ecological processes happening at the level of strains drove the observed change in the genetic composition of this species; and in particular, the change can be attributed to a dramatic shift in abundance of just one of the two populations initially

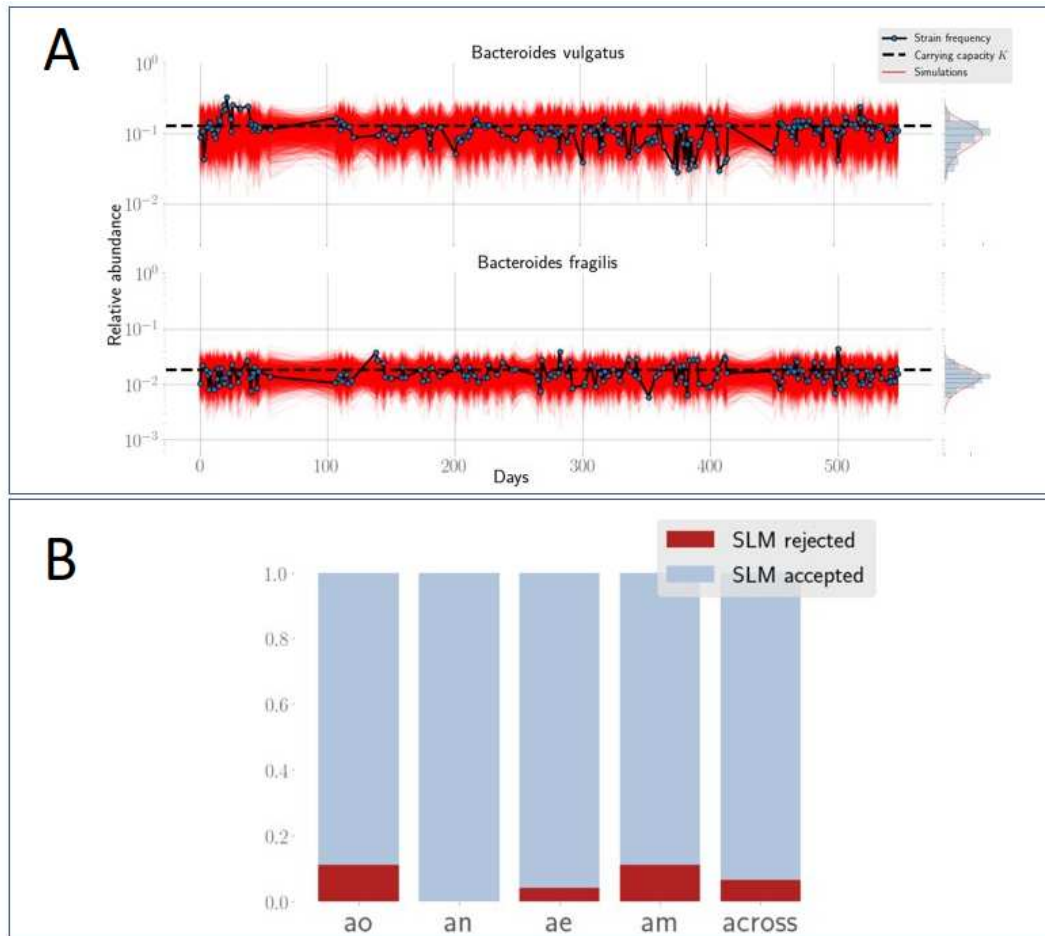


Figure 2. **A)** Simulations of the SLM associated with each strain, in red, capture the behavior of the real data at multiple time scales. Short-term increases and decreases are followed by returns to the long-term carrying capacity K . At far right, in blue, are histograms of the strains' abundance, and overlaid in red is the Gamma stationary distribution of abundances predicted by the SLM, described in equation 1. **B)** The percentage (y-axis) of strains for hosts *am*, *ae*, *ao*, and *an* passing the SLM goodness of fit test. A high proportion of strains pass the test—89% in *ao*, 100% in *an*, 96% in *ae*, and 89% in *am*. Across all four hosts, 94% of strains pass the test.

present. Despite this shift, both strains were detectable at all time points. Though the SLM was rejected in several other populations, *F. prausnitzii* was the only species which simultaneously experienced a statistically significant change in genetic diversity. 158
159
160

Together, these results indicate that the great majority of strains in the gut microbial community fluctuate around fixed average carrying capacities for periods of years, at least. 161
162

Macroecology of strains 163

While we have already seen that individual strains tend to be well described by an SLM, we show in the following section that the size of fluctuations across strains are strongly constrained. In many kinds of 164
165

microbial ecosystems, including the human gut, species have been shown to broadly obey macroecological laws [1, 45]. We show here that these patterns equally well characterize patterns of variation in the abundance of strains across our cohort.

The first pattern examined is a power law scaling between the mean and variance of abundance, known in ecology as Taylor's Law, and can be stated:

$$\sigma_{x_i}^2 \propto \langle x_i \rangle^\alpha \quad (3)$$

where $\langle x_i \rangle$ and $\sigma_{x_i}^2$ are the mean and variance of population x_i , respectively, and α is the scaling exponent of the power law. In communities where the relative scale of fluctuations is independent of population size—constant per-capita fluctuations— α will equal 2 [45]. We observed a Taylor's Law scaling with an exponent of $\alpha = 1.63$ among all strains (**Figure 3A**), closely mirroring previous findings at the species level [45].

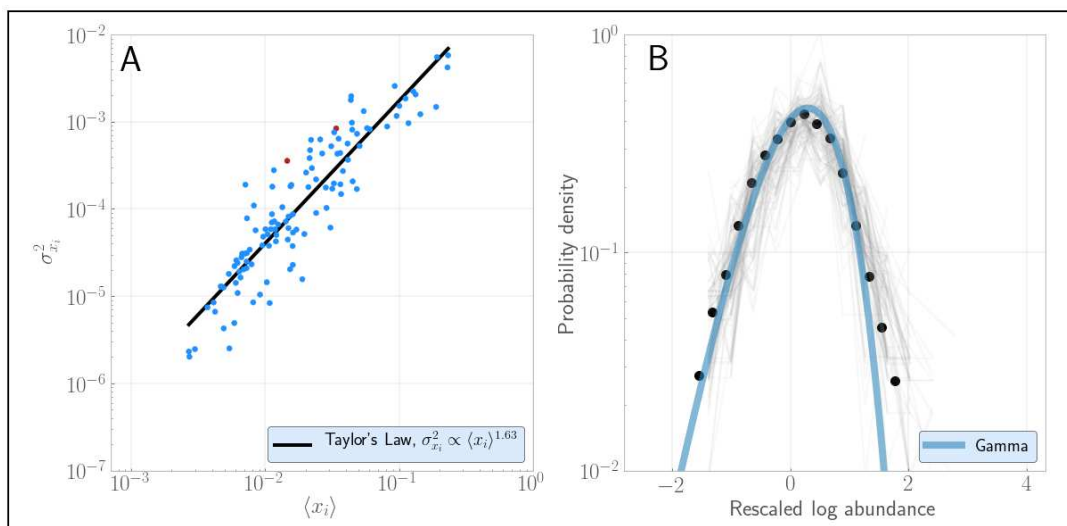


Figure 3. **A)** Strains obey Taylor's Law with exponent $\alpha = 1.63$. All strains are colored blue except the previously discussed strains belonging to *Faecalibacterium prausnitzii* in ao, which are colored red. **B)** The Gamma distribution describes the fluctuations in abundances of strains through time. To enable comparison across strains which have mean abundances ranging across several orders of magnitude, the AFD of each individual strain (grey lines) has been rescaled to have mean zero and unit variance. The black dots show the mean probability of a given rescaled abundance across strains.

The next pattern considered is the Gamma abundance fluctuation distribution (AFD), the overall distribution of abundances of a population through time. As discussed above, a population governed by stochastic logistic dynamics will tend towards a Gamma distribution of abundances over long timescales. Given the generally excellent fit of the SLM to the population time series, the abundances of strains might generically be expected to each individually follow a Gamma distribution. In (**Figure 3B**), we see that the distributions of strain abundances are indeed well described by a Gamma distribution; however, this Gamma is also conserved across strains—that is, all strains approximately lie (up to a scaling factor) along the same Gamma. Recalling that each SLM is uniquely determined by the mean and variance of population, it is apparent that the collapse of the AFDs to a single Gamma is in fact a consequence of the strong constraint Taylor's Law places on these quantities across strains.

The observed macroecological patterns continue to hold even when limiting our attention only to strains for which another strain of the same species is present (Supplemental Figure 4). Thus, two very broad macroecological laws observed at the species level in the human gut are also observed among strains, suggesting that the biotic and abiotic factors driving these patterns may act at the level of strains. 186
187
188
189

Discussion 190

In this study, we sought to characterize the typical within-species population dynamics in the human gut microbiome. Previous efforts have demonstrated that the genetic diversity within a host persists for multiple years for most species [24, 25]. We build on this result by demonstrating that intraspecies diversity tends to fluctuate around a long-term average value within a typical host on a time scale of several years. We show, crucially, that the abundance fluctuations of the vast majority of strains can be sufficiently described by a stochastic logistic model (SLM) of growth, a model which also recapitulates fluctuations at the species level [1, 6]. Furthermore, empirical patterns of strain abundance follow macroecological laws which have been previously demonstrated to hold at the species level [1, 6]. Together, our results suggest that the macroecological dynamics exhibited by species are recapitulated at the strain level. 191
192
193
194
195
196
197
198
199

While the SLM was able to sufficiently describe strain dynamics for the vast majority of strains across species, its success is not universal. One strain of *F. prausnitzii* is a noted exception, as its abundance decreased dramatically in abundance in a way that could not be explained by the stationary dynamics of the SLM. The directional change in abundance of this strain throws into relief the stability of the majority of the other strains—it is an exception that proves the rule, illustrating that strain dynamics might be quite different across strains, and that these differences can be detected by our test of the SLM. This example also brings to light an interesting tension in the interpretation of our results. Under the SLM, strains are expected to persist indefinitely. However, over the course of decades, much of the strain content of the adult gut is replaced [10, 15], suggesting that there is an additional timescale which is relevant for strain replacement. One hypothesis is that this timescale reflects a waiting time for large environmental perturbations, such as antibiotics [23, 32] or bowel cleanse [49], but this is just one of many hypotheses. Indeed, this hypothesis is partially challenged by [23], where the strain content of an adult gut was initially perturbed during a course of antibiotics, but ultimately recovered to its pretreatment state. This antibiotics study is a powerful demonstration of the stability of strains as ecological units, even in the face of large perturbations. Testing the possible explanations for the apparent discrepancy between years and decades-long population dynamics is an important problem to address with broad cohorts and extended timescales of observation. 200
201
202
203
204
205
206
207
208
209
210
211
212
213
214
215
216

Beyond the success of the SLM as an ecological model of strain dynamics in our cohort, the existence of many linked mutations segregating at intermediate frequencies across multiple species is qualitatively inconsistent with most standard population genetic models of microbial evolution [18]—particularly, models emphasizing directional selection or neutral evolution. However, the stability of both total genetic diversity and strain abundance belies the fact that SNVs likely continue to arise and fix within these populations even on the timescales examined here. While strain dynamics may often be suitably described by a time invariant model, these populations are not genetically static. Recent work has shown that variants arise and fix within populations in the gut microbiome regularly over months to years [10, 15, 30] 217
218
219
220
221
222
223
224
225
226

How evolution impacts the ecological dynamics of strains and how in turn these ecological dynamics constrain and channel evolution, is an active area of research [18]. In the context of the SLM, these 227
228
229
230
231
232
233
234
235
236
237
238
239
240
241
242
243
244
245
246
247
248
249
250
251
252
253
254
255
256
257
258
259
260
261
262
263
264
265
266
267
268
269
270
271
272
273
274
275
276
277
278
279
280
281
282
283
284
285
286
287
288
289
290
291
292
293
294
295
296
297
298
299
300
301
302
303
304
305
306
307
308
309
310
311
312
313
314
315
316
317
318
319
320
321
322
323
324
325
326
327
328
329
330
331
332
333
334
335
336
337
338
339
340
341
342
343
344
345
346
347
348
349
350
351
352
353
354
355
356
357
358
359
360
361
362
363
364
365
366
367
368
369
370
371
372
373
374
375
376
377
378
379
380
381
382
383
384
385
386
387
388
389
390
391
392
393
394
395
396
397
398
399
400
401
402
403
404
405
406
407
408
409
410
411
412
413
414
415
416
417
418
419
420
421
422
423
424
425
426
427
428
429
430
431
432
433
434
435
436
437
438
439
440
441
442
443
444
445
446
447
448
449
450
451
452
453
454
455
456
457
458
459
460
461
462
463
464
465
466
467
468
469
470
471
472
473
474
475
476
477
478
479
480
481
482
483
484
485
486
487
488
489
490
491
492
493
494
495
496
497
498
499
500
501
502
503
504
505
506
507
508
509
510
511
512
513
514
515
516
517
518
519
520
521
522
523
524
525
526
527
528
529
530
531
532
533
534
535
536
537
538
539
540
541
542
543
544
545
546
547
548
549
550
551
552
553
554
555
556
557
558
559
5510
5511
5512
5513
5514
5515
5516
5517
5518
5519
5520
5521
5522
5523
5524
5525
5526
5527
5528
5529
5530
5531
5532
5533
5534
5535
5536
5537
5538
5539
5540
5541
5542
5543
5544
5545
5546
5547
5548
5549
5550
5551
5552
5553
5554
5555
5556
5557
5558
5559
55510
55511
55512
55513
55514
55515
55516
55517
55518
55519
55520
55521
55522
55523
55524
55525
55526
55527
55528
55529
55530
55531
55532
55533
55534
55535
55536
55537
55538
55539
55540
55541
55542
55543
55544
55545
55546
55547
55548
55549
55550
55551
55552
55553
55554
55555
55556
55557
55558
55559
55560
55561
55562
55563
55564
55565
55566
55567
55568
55569
55570
55571
55572
55573
55574
55575
55576
55577
55578
55579
55580
55581
55582
55583
55584
55585
55586
55587
55588
55589
55590
55591
55592
55593
55594
55595
55596
55597
55598
55599
555100
555101
555102
555103
555104
555105
555106
555107
555108
555109
555110
555111
555112
555113
555114
555115
555116
555117
555118
555119
555120
555121
555122
555123
555124
555125
555126
555127
555128
555129
555130
555131
555132
555133
555134
555135
555136
555137
555138
555139
555140
555141
555142
555143
555144
555145
555146
555147
555148
555149
555150
555151
555152
555153
555154
555155
555156
555157
555158
555159
555160
555161
555162
555163
555164
555165
555166
555167
555168
555169
555170
555171
555172
555173
555174
555175
555176
555177
555178
555179
555180
555181
555182
555183
555184
555185
555186
555187
555188
555189
555190
555191
555192
555193
555194
555195
555196
555197
555198
555199
555200
555201
555202
555203
555204
555205
555206
555207
555208
555209
555210
555211
555212
555213
555214
555215
555216
555217
555218
555219
555220
555221
555222
555223
555224
555225
555226
555227
555228
555229
555230
555231
555232
555233
555234
555235
555236
555237
555238
555239
555240
555241
555242
555243
555244
555245
555246
555247
555248
555249
555250
555251
555252
555253
555254
555255
555256
555257
555258
555259
555260
555261
555262
555263
555264
555265
555266
555267
555268
555269
555270
555271
555272
555273
555274
555275
555276
555277
555278
555279
555280
555281
555282
555283
555284
555285
555286
555287
555288
555289
555290
555291
555292
555293
555294
555295
555296
555297
555298
555299
555300
555301
555302
555303
555304
555305
555306
555307
555308
555309
555310
555311
555312
555313
555314
555315
555316
555317
555318
555319
555320
555321
555322
555323
555324
555325
555326
555327
555328
555329
555330
555331
555332
555333
555334
555335
555336
555337
555338
555339
555340
555341
555342
555343
555344
555345
555346
555347
555348
555349
555350
555351
555352
555353
555354
555355
555356
555357
555358
555359
555360
555361
555362
555363
555364
555365
555366
555367
555368
555369
555370
555371
555372
555373
555374
555375
555376
555377
555378
555379
555380
555381
555382
555383
555384
555385
555386
555387
555388
555389
555390
555391
555392
555393
555394
555395
555396
555397
555398
555399
555400
555401
555402
555403
555404
555405
555406
555407
555408
555409
555410
555411
555412
555413
555414
555415
555416
555417
555418
555419
555420
555421
555422
555423
555424
555425
555426
555427
555428
555429
555430
555431
555432
555433
555434
555435
555436
555437
555438
555439
555440
555441
555442
555443
555444
555445
555446
555447
555448
555449
555450
555451
555452
555453
555454
555455
555456
555457
555458
555459
555460
555461
555462
555463
555464
555465
555466
555467
555468
555469
555470
555471
555472
555473
555474
555475
555476
555477
555478
555479
555480
555481
555482
555483
555484
555485
555486
555487
555488
555489
555490
555491
555492
555493
555494
555495
555496
555497
555498
555499
555500
555501
555502
555503
555504
555505
555506
555507
555508
555509
555510
555511
555512
555513
555514
555515
555516
555517
555518
555519
555520
555521
555522
555523
555524
555525
555526
555527
555528
555529
555530
555531
555532
555533
555534
555535
555536
555537
555538
555539
555540
555541
555542
555543
555544
555545
555546
555547
555548
555549
555550
555551
555552
555553
555554
555555
555556
555557
555558
555559
555560
555561
555562
555563
555564
555565
555566
555567
555568
555569
555570
555571
555572
555573
555574
555575
555576
555577
555578
555579
555580
555581
555582
555583
555584
555585
555586
555587
555588
555589
555590
555591
555592
555593
555594
555595
555596
555597
555598
555599
5555100
5555101
5555102
5555103
5555104
5555105
5555106
5555107
5555108
5555109
5555110
5555111
5555112
5555113
5555114
5555115
5555116
5555117
5555118
5555119
5555120
5555121
5555122
5555123
5555124
5555125
5555126
5555127
5555128
5555129
5555130
5555131
5555132
5555133
5555134
5555135
5555136
5555137
5555138
5555139
5555140
5555141
5555142
5555143
5555144
5555145
5555146
5555147
5555148
5555149
5555150
5555151
5555152
5555153
5555154
5555155
5555156
5555157
5555158
5555159
5555160
5555161
5555162
5555163
5555164
5555165
5555166
5555167
5555168
5555169
5555170
5555171
5555172
5555173
5555174
5555175
5555176
5555177
5555178
5555179
5555180
5555181
5555182
5555183
5555184
5555185
5555186
5555187
5555188
5555189
5555190
5555191
5555192
5555193
5555194
5555195
5555196
5555197
5555198
5555199
5555200
5555201
5555202
5555203
5555204
5555205
5555206
5555207
5555208
5555209
5555210
5555211
5555212
5555213
5555214
5555215
5555216
5555217
5555218
5555219
5555220
5555221
5555222
5555223
5555224
5555225
5555226
5555227
5555228
5555229
5555230
5555231
5555232
5555233
5555234
5555235
5555236
5555237
5555238
5555239
5555240
5555241
5555242
5555243
5555244
5555245
5555246
5555247
5555248
5555249
5555250
5555251
5555252
5555253
5555254
5555255
5555256
5555257
5555258
5555259
5555260
5555261
5555262
5555263
5555264
5555265
5555266
5555267
5555268
5555269
5555270
5555271
5555272
5555273
5555274
5555275
5555276
5555277
5555278
5555279
5555280
5555281
5555282
5555283
5555284
5555285
5555286
5555287
5555288
5555289
5555290
5555291
5555292
5555293
5555294
5555295
5555296
5555297
5555298
5555299
5555300
5555301
5555302
5555303
5555304
5555305
5555306
5555307
5555308
5555309
5555310
5555311
5555312
5555313
5555314
5555315
5555316
5555317
5555318
5555319
5555320
5555321
5555322
5555323
5555324
5555325
5555326
5555327
5555328
5555329
5555330
5555331
5555332
5555333
5555334
5555335
5555336
5555337
5555338
5555339
5555340
5555341
5555342
5555343
5555344
5555345
5555346
5555347
5555348
5555349
5555350
5555351
5555352
5555353
5555354
5555355
5555356
5555357
5555358
5555359
5555360
5555361
5555362
5555363
5555364
5555365
5555366
5555367
5555368
5555369
5555370
5555371
5555372
5555373
5555374
5555375
5555376
5555377
5555378
5555379
5555380
5555381
5555382
5555383
5555384
5555385
5555386
5555387
5555388
5555389
5555390
5555391
5555392
5555393
5555394
5555395
5555396
5555397
5555398
5555399
5555400
5555401
5555402
5555403
5555404
5555405
5555406
5555407
5555408
5555409
5555410
5555411
5555412
5555413
5555414
5555415
5555416
5555417
5555418
5555419
5555420
5555421
5555422
5555423
5555424
5555425
5555426
5555427
5555428
5555429
5555430
5555431
5555432
5555433
5555434
5555435
5555436
5555437
5555438
5555439
5555440
5555441
5555442
5555443
5555444
5555445
5555446
5555447
5555448
5555449
5555450
5555451
5555452
5555453
5555454
5555455
5555456
5555457
5555458
5555459
5555460
5555461
5555462
5555463
5555464
5555465
5555466
5555467
5555468
5555469
5555470
5555471
5555472
5555473
5555474
5555475
5555476
5555477
5555478
5555479
5555480
5555481
555548

eco-evolutionary feedbacks can be viewed as tuning a strain's carrying capacity K , growth rate $\frac{1}{\tau}$, and
227
sensitivity of the growth rate to environmental perturbation σ . Naively, it is expected that evolution would
228
tend to increase carrying capacity while minimizing the sensitivity of growth to abiotic fluctuations, but
229
evolutionary modifications driving changes in one quantity may affect the other. The observed power-law
230
scaling between the mean and variance in abundance (Taylor's Law) is, in essence, a constraint on K given
231
 σ , and vice versa. The SLM thus not only describes ecological dynamics, but also, in conjunction with the
232
empirical observation of macroecological laws, provides a useful framework for investigating the ecological
233
effects of adaptation.
234

How and why closely related strains stably coexist in the human gut is one of the central biological
235
questions raised by these results. Spatial segregation between strains, perhaps occupying different colonic
236
crypts, could underlie the observed pattern of strain coexistence [20, 27], much as it does among
237
Cutibacterium acnes strains inhabiting different pores on the facial microbiome [42]. However, spatial
238
structure is far from the only mechanism that can foster coexistence between strains. Coexisting strains
239
have been reported in well-mixed laboratory evolution experiments [4, 8, 55]. In these experiments, strains
240
coexist by finely partitioning some aspect of the abiotic environment or by engaging in ecological
241
interactions (e.g. cross-feeding), or by some combination of both. Recent work has shown that
242
consumer-resource models, which describe the flux of metabolites through a community and the growth of
243
community members on these metabolites, can recapitulate a large number of species-level macroecological
244
properties of microbial communities with only a small number of input parameters [29, 31, 44]. Investigating
245
which of these scenarios promotes strain coexistence will be an interesting avenue for future research.
246

Finally, the success of the SLM at the strain and species level raises questions regarding which scale
247
ought to be the focus of ecological investigations. The ambiguity surrounding the bacterial species concept
248
is well known [34] and reasonable alternatives have been proposed [19], but operationally species are,
249
nonetheless, the predominant focus of attention in microbial ecology. This focus is reasonable, as
250
within-host strain structure is a comparatively recent discovery [10, 28, 54] and 16S rRNA sequencing
251
provides an inexpensive high-throughput means to examine community dynamics through OTUs.
252
Regardless, the recapitulation of species-level macroecological dynamics at the level of strains calls into
253
question the disproportionate focus on species as the primary locus of attention in characterizing
254
community structure and dynamics. Instead, it is reasonable to propose that for the human gut, and
255
perhaps other microbial ecosystems, strains are an ecologically relevant unit.
256

Methods

Data and metagenomic pipeline

We analyzed shotgun metagenomic sequence data from a panel of stool samples from 4 healthy human
259
subjects [21]. The four hosts examined—*ae*, *am*, *an* and *ao*—were sampled longitudinally over the course of
260
between six months and two years, and none of the hosts experienced any disturbances such as antibiotics
261
or bowel cleanse. We excluded one sample from host *ae* which appeared to be mislabelled and/or
262
contaminated (Supplemental Figure 5). We used a reference-based approach to analyze metagenomic
263
sequences, calling SNVs and gene content, as well as species abundances, using the software MIDAS [13].
264

Calculating diversity statistics

Nucleotide diversity π is a classical population genetic measure of polymorphism, representing the average number of pairwise difference between randomly chosen members of a population. To determine π , we used the estimator:

$$\pi = \frac{1}{|G|} \sum_{i=1}^{|G|} 2p_i(1 - p_i) \quad (4)$$

where p_i is the frequency of the reference allele at site i , and $|G|$ is the total number of sites in the genome. This quantity was calculated after first excluding sites with low read depth ($< 5x$), as reliable estimates of true allele frequency cannot be made for such sites.

Similarly, π_{BT} , the diversity between timepoints, was calculate

$$\pi_{BT} = \frac{1}{|G|} \sum_{i=1}^{|G|} (p_{1i}(1 - p_{2i}) + p_{2i}(1 - p_{1i})) \quad (5)$$

where p_{1i} is the frequency of the reference allele at site i in sample 1, and p_{2i} its frequency in sample 2.

Lastly, to determine π_{BH} , the diversity between hosts for a give species, we used shotgun data from the Human Microbiome Project (HMP), processed through the same metagenomic pipeline as above [17]. HMP was chosen as an due to the large number of samples (469, in total) and high coverage. π_{BH} was calculated as the mean pairwise diversity (Equation 5) between all pairs of samples of a species found in different hosts.

Permutation test

To assess whether diversity tended to systematically increase or decrease through time for species in our cohort, we performed a standard permutation test [51]. First, a linear regression was performed on β_i . The observed time series of π and π_{BT} were permuted with respect to temporal order 1000 times, and for each permutation, a linear regression was fit. The slopes of these regressions— $\beta_i^1, \beta_i^2, \dots, \beta_i^{1000}$ —are centered around 0, and form a null distribution for the true slope under the assumption that there are no long-term temporal trends in the data. We rejected the null hypothesis at a signficance level of 5%.

Strain inference

To infer strains, we used a recently published algorithm [23] developed specifically to detect strains in metagenomic timecourse data. At a high level, this algorithm identifies clusters of SNVs that have similar allele frequency trajectories across a longitudinal panel of samples, modulo binomial sampling noise at each timepoint. Such clusters are expected when alleles at different loci are linked on the same genetic background (and therefore have the same true frequency at any timepoint), but differ in their observed frequencies due to finite sampling. Once SNVs have been clustered, the centroid of each cluster of trajectories is taken to be an estimator of the underlying relative frequency of the strain.

SLM

To simulate the SLM, we used the Euler-Maruyama method:

$$X(t + \delta t) = X(t) + \frac{x(t)}{\tau_i} \left(1 - \frac{x(t)}{K}\right) \delta t + \sqrt{\frac{\sigma}{\tau}} x(t) Z_t \sqrt{\delta t} \quad (6)$$

where Z_t is a standard normal random variable. In simulations, we set $\delta t = \frac{1}{1000}$.

The SLM associated with population i depends on three parameters: K_i , σ_i , and τ_i . K_i and σ_i are not fit, but rather are determined directly from the mean and variance of the actual time series using the formulae:

$$\sigma_i = \frac{2}{\frac{\langle x_i \rangle^2}{\sigma_{x_i}^2} - 1}, \quad K_i = \frac{\langle x_i \rangle}{1 - \frac{\sigma_i}{2}} \quad (7)$$

where $\langle x_i \rangle$ is the mean abundance of the population and $\sigma_{x_i}^2$ is its variance. The parameter τ_i was held constant ($\tau_i = 1$) for all strains to avoid overfitting.

To calculate $\sigma_{x_i}^2$, we used the sampling-corrected estimate of the true variance as done in [1] and [43]:

$$\sigma_{x_i}^2 = \frac{1}{|T|} \sum_{t \in T} \frac{x_i(t)(x_i(t) - 1)}{N(t)(N(t) - 1)} - \left(\frac{1}{|T|} \sum_{t \in T} \frac{x_i(t)}{N(t)} \right)^2. \quad (8)$$

where T is the set of timepoints for which strain i is present, and $N(t)$ is the total abundance of all species present in the sample at timepoint t , as determined by MIDAS.

Goodness of fit test

The goodness of fit test for the SLM was adopted from the test described in [50]. The null hypothesis of this test is that the SLM with the parameters determined in the previous section generated the observed time series.

The test is performed as follows. Suppose that $x(t_0), x(t_1), \dots, x(t_{T-1})$ are the T observations of strain's abundance, at times t_0, t_1, \dots, t_{T-1} . M simulations are performed using the Euler-Maruyama procedure described in equation (6), above, from time t_{i-1} until time t_i , starting at initial abundance x_{i-1} .

Let $X_i^{(m)}$ be the the m^{th} simulated value at time t_i for $m = 1, 2, \dots, M$. Define r_i to be the number of $X_i^{(m)} < x(t_i)$ —that is, the number of simulations of the process from t_{i-1} to t_i in which the final simulated value was less than the true abundance.

Under the null hypothesis, the r_i are equally likely to take any value between 0 and M . Therefore, we perform a χ^2 goodness-of-fit test to determine if the r_i follow a uniform distribution on $0, 1, \dots, M$, obtaining a p-value. We repeat this whole process 1000 times for each time series, and take the true p-value to be the median p-value across all runs. We rejected the null hypothesis at a significance level of 5%.

Acknowledgments

We thank Colin Kremer for his critical feedback on this manuscript, and Van Savage for early discussions on this work. We also thank members of the Garud lab for their feedback. This work was supported by the NSF Postdoctoral Research Fellowships in Biology Program under Grant No. 2010885 (W.R.S.). as well as the the Paul Allen Foundation, the UCLA Hellman Fellowship, and the Research Corporation for Science Advancement (N.R.G.).

References

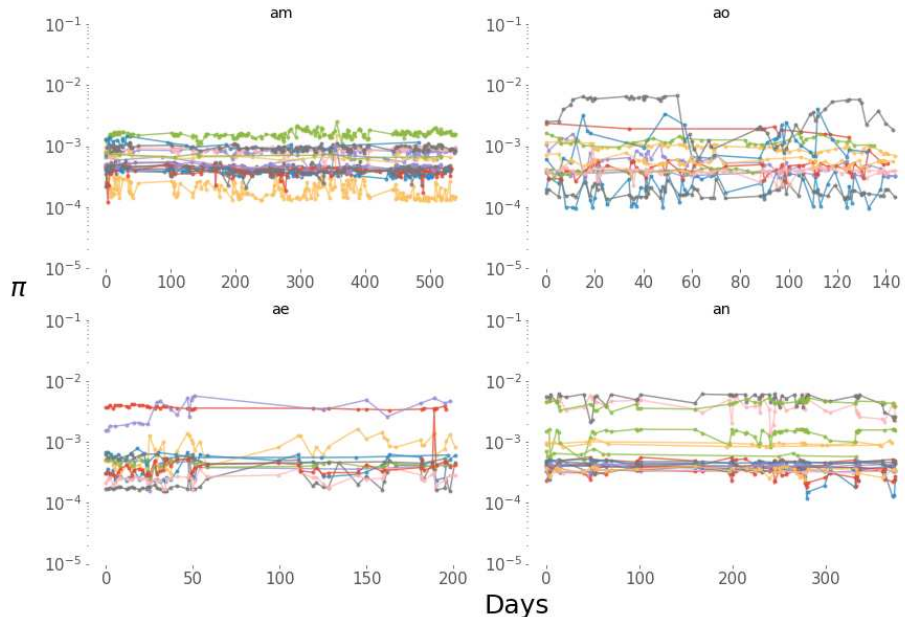
1. Grilli, J. Macroecological laws describe variation and diversity in microbial communities. *Nat Commun* 11,4743 (2020).
2. Smith, J. Maynard, et al. “How clonal are bacteria?” *Proceedings of the National Academy of Sciences* 90.10 (1993): 4384-4388.
3. Shapiro, B. Jesse. “How clonal are bacteria over time?.” *Current opinion in microbiology* 31 (2016): 116-123.
4. Lenski, R. “Experimental evolution and the dynamics of adaptation and genome evolution in microbial populations.” *ISME J* 11, 2181–2194 (2017).
5. Chen, Lianmin, et al. “The long-term genetic stability and individual specificity of the human gut microbiome.” *Cell* 184.9 (2021): 2302-2315.
6. Descheemaeker L., De Buyl S. “Stochastic logistic models reproduce experimental time series of microbial communities.” *Elife* (2020)
7. Ho, Po-Yi, Benjamin H. Good, and Kerwyn Huang. “Competition for fluctuating resources reproduces statistics of species abundance over time across wide-ranging microbiotas.” *bioRxiv* (2021).
8. Goyal, A., Bittleson, L., Leventhal, G., Lu, L., Cordero, X. “Interactions between strains govern the eco-evolutionary dynamics of microbial communities.” *bioRxiv* (2021).
9. Verster A; Ross B; Radey M; Bao Y; Goodman A; Mougous J; Borenstein E. “The Landscape of Type VI Secretion across Human Gut Microbiomes Reveals Its Role in Community Composition.” *Cell Host Microbe* (2017).
10. Garud N; Good B; Hallatschek O; Pollard K. “Evolutionary dynamics of bacteria in the gut microbiome within and across hosts.” *PLOS Biology* (2019).
11. Li, Simone S., et al. “Durable coexistence of donor and recipient strains after fecal microbiota transplantation.” *Science* 352.6285 (2016): 586-589.
12. Smillie C. *et al.* “Strain Tracking Reveals the Determinants of Bacterial Engraftment in the Human Gut Following Fecal Microbiota Transplantation.” *Cell Host Microbe*. (2018).

13. Nayfach, S., Rodriguez-Mueller, B., Garud, N., & Pollard, K. S. "An integrated metagenomics pipeline for strain profiling reveals novel patterns of bacterial transmission and biogeography." *Genome research*, 26(11), 1612-1625. (2016).
14. Shoemaker, W. R., Locey, K. J., & Lennon, J. T. "A macroecological theory of microbial biodiversity." *Nature ecology & evolution*, 1(5), 1-6. (2017)
15. Yaffe, Eitan, and David A. Relman. "Tracking microbial evolution in the human gut using Hi-C reveals extensive horizontal gene transfer, persistence and adaptation." *Nature microbiology* 5.2 (2020): 343-353.
16. Russell, Shelbi L., and Colleen M. Cavanaugh. "Intrahost genetic diversity of bacterial symbionts exhibits evidence of mixed infections and recombinant haplotypes." *Molecular Biology and Evolution* 34.11 (2017): 2747-2761.
17. Lloyd-Price, J. *et al.* "The integrative human microbiome project." *Nature* (2019).
18. Good, Benjamin H., Stephen Martis, and Oskar Hallatschek. "Adaptation limits ecological diversification and promotes ecological tinkering during the competition for substitutable resources." *Proceedings of the National Academy of Sciences* 115.44 (2018): E10407-E10416.
19. Tikhonov, Mikhail. "Theoretical microbial ecology without species." *Physical Review E* 96.3 (2017): 032410.
20. Tropini, Carolina, et al. "The gut microbiome: connecting spatial organization to function." *Cell host & microbe* 21.4 (2017): 433-442.
21. Poyet, M., Groussin, M., Gibbons, S.M. *et al.* "A library of human gut bacterial isolates paired with longitudinal multiomics data enables mechanistic microbiome research." *Nat Med* 25, 1442–1452 (2019).
22. Voigt, A.Y., Costea, P.I., Kultima, J.R. *et al.* "Temporal and technical variability of human gut metagenomes." *Genome Biol* 16, 73 (2015).
23. Roodgar, M., Good, B. H., Garud, N. R., Martis, S., Avula, M., Zhou, W., Snyder, M. P. *et al.* "Longitudinal linked read sequencing reveals ecological and evolutionary responses of a human gut microbiome during antibiotic treatment." *Genome Research*. (2021).
24. Schloissnig, S., Arumugam, M., Sunagawa, S., Mitreva, M., Tap, J., Zhu, A., Bork, P. "Genomic variation landscape of the human gut microbiome." *Nature*, 493(7430), 45-50. (2013).
25. Faith, J. J., Guruge, J. L., Charbonneau, M., Subramanian, S., Seedorf, H., Goodman, A. L., Gordon, J. I. "The long-term stability of the human gut microbiota." *Science*, 341(6141). (2013)
26. Hubbell, Stephen P. "The unified neutral theory of biodiversity and biogeography" (MPB-32). Princeton University Press, 2011.
27. Karita, Yuya, David T. Limmer, and Oskar Hallatschek. "Scale-dependent tipping points of bacterial colonization resistance." bioRxiv (2021).

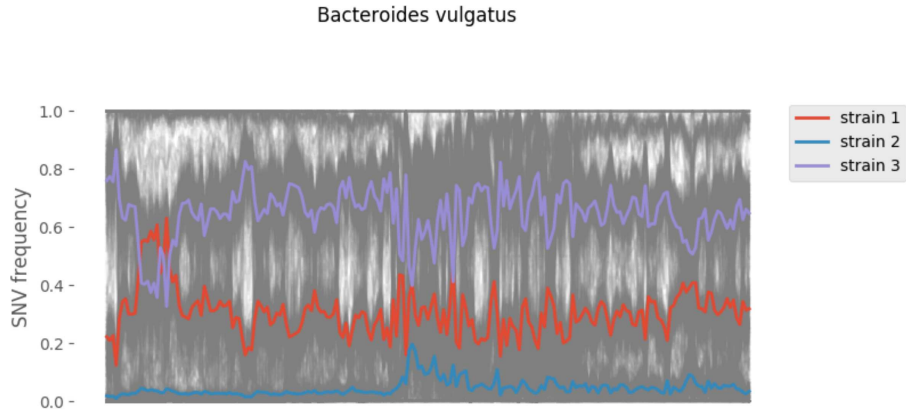
28. Zheng, W, et al. "Microbe-seq: high-throughput, single-microbe genomics with strain resolution, applied to a human gut microbiome." *bioRxiv* (2020)
29. Goldford, Joshua E., et al. "Emergent simplicity in microbial community assembly." *Science* 361.6401 (2018): 469-474.
30. Zhao, S., et al. "Adaptive evolution within gut microbiomes of healthy people." *Cell host microbe*, 25(5), 656-667. (2019).
31. Marsland III, Robert, et al. "Available energy fluxes drive a transition in the diversity, stability, and functional structure of microbial communities." *PLoS computational biology* 15.2 (2019): e1006793.
32. Korpela, Katri, et al. "Selective maternal seeding and environment shape the human gut microbiome." *Genome research* 28.4 (2018): 561-568.
33. Lloyd-Price, J., Abu-Ali, G. Huttenhower, C. "The healthy human microbiome." *Genome Med* 8, 51 (2016). <https://doi.org/10.1186/s13073-016-0307-y>
34. Tang, Le et al. "Defining natural species of bacteria: clear-cut genomic boundaries revealed by a turning point in nucleotide sequence divergence." *BMC genomics* vol. 14 489. 18 Jul. 2013, doi:10.1186/1471-2164-14-489
35. Cordero, Otto X., and Martin F. Polz. "Explaining microbial genomic diversity in light of evolutionary ecology." *Nature Reviews Microbiology* 12.4 (2014): 263-273.
36. Lewontin, Richard C. The genetic basis of evolutionary change. Vol. 560. New York: Columbia University Press, 1974.
37. Murray, C.S., Gao, Y. Wu, M. "Re-evaluating the evidence for a universal genetic boundary among microbial species." *Nat Commun* 12, 4059 (2021). <https://doi.org/10.1038/s41467-021-24128-2>
38. Cordero, O., Polz, M. Explaining microbial genomic diversity in light of evolutionary ecology. *Nat Rev Microbiol* 12, 263–273 (2014). <https://doi.org/10.1038/nrmicro3218>
39. Utter, Daniel R., Colleen M. Cavanaugh, and Gary G. Borisy. "Gene-and genome-centric dynamics shape the diversity of oral bacterial populations." *bioRxiv* (2021).
40. Leventhal, Gabriel E., et al. "Strain-level diversity drives alternative community types in millimetre-scale granular biofilms." *Nature microbiology* 3.11 (2018): 1295-1303.
41. Mark Welch, Jessica L., et al. "Dynamics of tongue microbial communities with single-nucleotide resolution using oligotyping." *Frontiers in microbiology* 5 (2014): 568.
42. Conwill, Arolyn, et al. "Anatomy promotes neutral coexistence of strains in the human skin microbiome." *bioRxiv* (2021).
43. Zaoli, Silvia, and Jacopo Grilli. "A macroecological description of alternative stable states reproduces intra-and inter-host variability of gut microbiome." *bioRxiv* (2021).

44. Ho, Po-Yi, Benjamin H. Good, and Kerwyn Huang. "Competition for fluctuating resources reproduces statistics of species abundance over time across wide-ranging microbiotas." *bioRxiv* (2021).
45. Ji, Brian W., et al. "Macroecological dynamics of gut microbiota." *Nature microbiology* 5.5 (2020): 768-775.
46. Rosen, Michael J., et al. "Fine-scale diversity and extensive recombination in a quasisexual bacterial population occupying a broad niche." *Science* 348.6238 (2015): 1019-1023.
47. Kashtan, Nadav, et al. "Single-cell genomics reveals hundreds of coexisting subpopulations in wild *Prochlorococcus*." *Science* 344.6182 (2014): 416-420.
48. Bak, Jakob, Henrik Madsen, and Henrik Aalborg Nielsen. "Goodness of fit of stochastic differential equations." *Symposium i Anvendt Statistik*. Copenhagen Business School Copenhagen, Denmark, 1999.
49. Tropini, Carolina, et al. "Transient osmotic perturbation causes long-term alteration to the gut microbiota." *Cell* 173.7 (2018): 1742-1754.
50. Allen, Edward. Modeling with Itô stochastic differential equations. Vol. 22. Springer Science Business Media, 2007.
51. Anderson, Marti J., and John Robinson. "Permutation tests for linear models." *Australian New Zealand Journal of Statistics* 43.1 (2001): 75-88.
52. Martinson JNV, Pinkham NV, Peters GW, Cho H, Heng J, Rauch M, et al. "Rethinking gut microbiome residency and the Enterobacteriaceae in healthy human adults." *ISME J.* 2019
53. Franzosa, Eric A., et al. "Identifying personal microbiomes using metagenomic codes." *Proceedings of the National Academy of Sciences* 112.22 (2015): E2930-E2938.
54. Truong, Duy Tin, et al. "Microbial strain-level population structure and genetic diversity from metagenomes." *Genome research* 27.4 (2017): 626-638.
55. Helling, Robert B., Christopher N. Vargas, and Julian Adams. "Evolution of *Escherichia coli* during growth in a constant environment." *Genetics* 116.3 (1987): 349-358.
56. Ghoul, Melanie, and Sara Mitri. "The ecology and evolution of microbial competition." *Trends in microbiology* 24.10 (2016): 833-845.
57. Verster, Adrian J., and Elhanan Borenstein. "Competitive lottery-based assembly of selected clades in the human gut microbiome." *Microbiome* 6.1 (2018): 1-17.

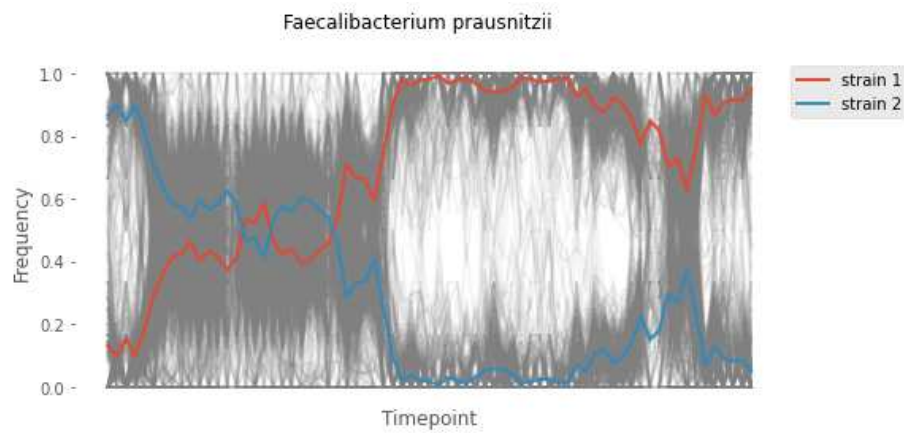
Supplementary Information



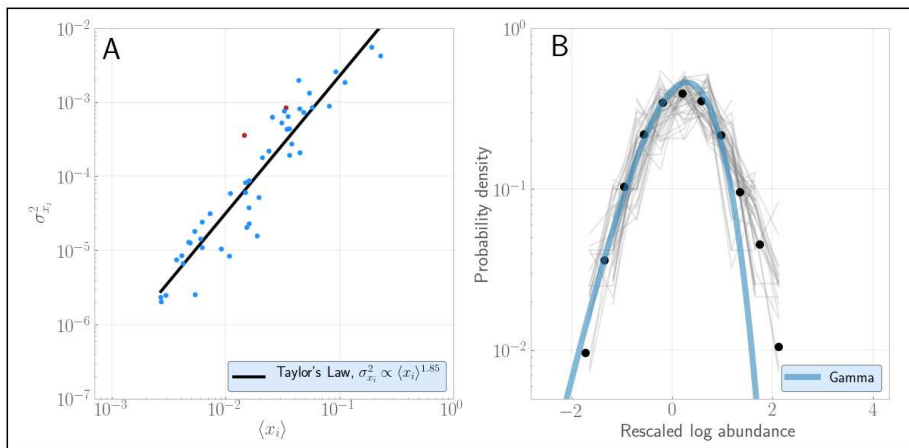
Supplementary Figure 1: Nucleotide diversity π for each species for which SNVs could be inferred, grouped by host. Each color represents a different species. Throughout the course of the sampling period, π undergoes large fluctuations in some species. However, in 55 of 64 cases, these fluctuations show no directional trend significantly different from 0, according to our permutation test.



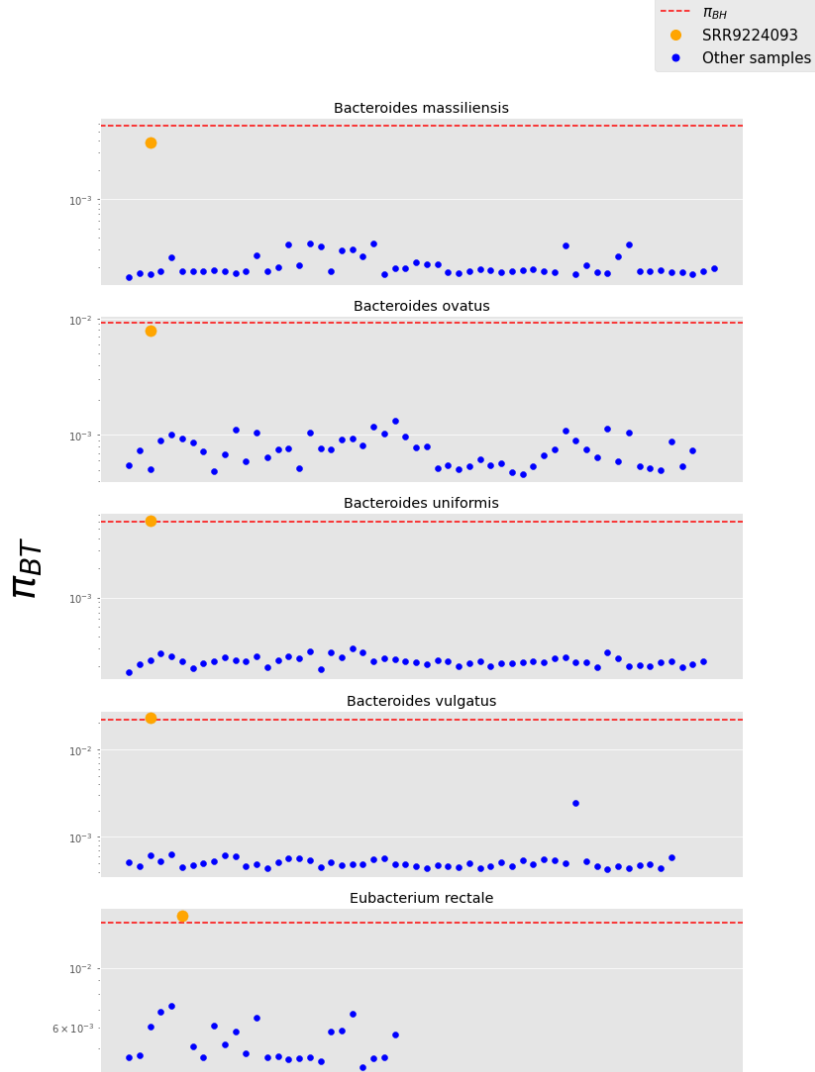
Supplementary Figure 2: Unphased allelic trajectories in *B. vulgatus* in host *am* (grey lines), and imputed strain frequencies. After phasing alleles to strains, only two of the clusters of SNVs remain visible.



Supplementary Figure 3: Two strains of *F. prausnitzii* present in host *ao* underwent a partial strain displacement event. In grey are the unphased trajectories of all SNPs detected throughout the sampling period. In red and blue are the inferred underlying strain frequencies detected after clustering SNP trajectories (Methods).



Supplementary Figure 4: The macroecological laws plotted only for strains belonging to species which harbor more than one strain. The red points in **A**, corresponding to the two strains of *F. prausnitzii* in host *ao*, are clear outliers, as expected given the partial strain replacement event these strains underwent. While the slope of the Taylor's Law exponent increased from 1.63 to 1.85 when considering only these strains, the power law scaling of the variance in abundance with the mean still holds. Similarly, the Gamma AFD still provides a good approximation to the true (rescaled) strain AFDs.



Supplementary Figure 5: One sample, SRR9224093, was removed from our analysis due to a possible mislabelling or contamination, which was noticed while performing this analysis. This sample was labelled to have come from host *ae*. Here, each blue dot represents π_{BT} between each sample from that host and a reference sample from host *ae* (the earliest sample detected for that species in this host). Only those species with more than three samples are plotted. SRR9224093 (orange dot) shows anomalously high π_{BT} compared to other samples. In particular, π_{BT} approaches π_{BH} only for this sample across multiple species, indicating that the genetic content of this sample is as different from the others in this host as a sample chosen from a random other individual would be. The consistent elevation of π_{BT} across multiple species at only this sample suggests this sample may have been mislabelled, or else may have been partially contaminated.